

## Performance study and analysis between vector control and direct power control for DFIG based wind energy system

Gufran Nurettin\*, Ata Sevinç

Department of Electrical and Electronic Engineering, Kırıkkale University, Kırıkkale, TURKEY

Email\* : [ahghby@gmail.com](mailto:ahghby@gmail.com)

**Abstract** – This paper concentrates on analyzing the performance of the two most important techniques of independent active and reactive power control of the doubly-fed induction generator used in a variable speed wind power conversion system. In the first technique, the independent control of the active and reactive power is based on the vector control technique by the orientation of the stator voltage space vector using PI controllers; the decoupling components are deduced along with the  $d$ ,  $q$  axes; and the PI controllers' parameters are calculated from the mathematical model of the doubly-fed induction generator. Hysteresis controllers are utilized to designing a direct power control technique. The performances of the studied control methods are tested and compared via simulation results.

**Keywords:** Voltage Oriented Control, Direct Power Control, DFIG

Received: 13/07/2021 – Accepted: 05/12/2021

### I. Introduction

The main reason for the popularity of doubly-fed induction generators (DFIGs) in wind power implementations is the requirement for relatively small power converters. (Usually, 30% from the rated power of the machine) [1-2].

The Scherbius scheme was introduced by the 20th-century German engineer Arthur Scherbius that provides bidirectional power flow in the rotor circuit. Cycloconverter-based power converter topologies joined between the stator and the rotor was informed [3-4]. However, these converters produce high harmonics in the rotor current returned to the stator. These disadvantages can be overcome by employing two separated converters, a Rotor Side Converter (RSC) and a Grid Side Converter (GSC), which are attached back-to-back in the rotor side [5]. To achieve control of the DFIG system, the RSC and GSC can be commanded independently. In practical applications, the RSC can operate in complete separation from the GSC provided that a steady DC bus voltage is supplied by the GSC. Also, in most schemes, the RSC

operates commands are completely independent of the GSC by a separate control unit for each converter.

One of the conventional control methods in the literature is the vector control that was utilized in the DFIG system [6]. The vector control method employing PI controllers provides a less harmonic distortion and reduces the power ripple [7]. But it might be hard to set the PI gains correctly and its performance depends significantly on machine parameters. The vector control technique according to orientation frame can be classified as the stator flux-oriented control (FOC) [8] or grid voltage-oriented control (VOC) [9].

FOC techniques depend on the accuracy of the stator resistance values, integration problems also exist and extra low-pass filters are applied to precisely determine the stator flux [10]. The influence of the value of stator resistance in the flux calculation can be neglected using the VOC technique by adding a 90-phase variation to the voltage angle which can be obtained using a Phase-Locked Loop (PLL). This can produce an added coupling impact in Active and Reactive Power (ARP) control, which can be recompensed by applying extra controllers

in the external loop [11-12].

Another control technique in the literature is direct torque control (DTC). The RSC provides the necessary magnetizing current in the rotor windings to produce the needed ARP at the stator terminals. Furthermore, since the electromagnetic torque is concerning to the active power, it is reported that the electromagnetic torque and stator flux reference values are replaced by ARP reference values [13-14].

The direct power control (DPC) technique directly controls the ARP of the stator by applying the suitable voltage vector to the rotor. The errors between the reference ARPs and the estimated ARPs are handled by hysteresis controllers [15-18].

The DPC is distinguished by its simple structure, fast dynamic response and robustness to parameter changes, and not need to use rotor current control loops, but its disadvantages are the highly variable switching frequency.

In this study, first, the dynamic model of the DFIG is proffered. Then the vector control and direct power control techniques are studied. At last, the detailed simulation results are presented and discussed using MATLAB/SIMULINK for both techniques.

## II. The Dynamic Model of DFIG

The dynamic model of the DFIG in the synchronous reference frame dq can be described by the following equations:

$$\left. \begin{aligned} V_{sd} &= R_s i_{sd} + \frac{d\psi_{sd}}{dt} - \omega_s \psi_{sq} \\ V_{sq} &= R_s i_{sq} + \frac{d\psi_{sq}}{dt} + \omega_s \psi_{sd} \end{aligned} \right\} \quad (1)$$

$$\left. \begin{aligned} V_{rd} &= R_r i_{rd} + \frac{d\psi_{rd}}{dt} - (\omega_s - \omega_r) \psi_{rq} \\ V_{rq} &= R_r i_{rq} + \frac{d\psi_{rq}}{dt} + (\omega_s - \omega_r) \psi_{rd} \end{aligned} \right\} \quad (2)$$

The stator and rotor fluxes are related to the current by:

$$\left. \begin{aligned} \psi_{sd} &= L_s i_{sd} + L_m i_{rd} \\ \psi_{sq} &= L_s i_{sq} + L_m i_{rq} \end{aligned} \right\} \quad (3)$$

$$\left. \begin{aligned} \psi_{rd} &= L_r i_{rd} + L_m i_{sd} \\ \psi_{rq} &= L_r i_{rq} + L_m i_{sq} \end{aligned} \right\} \quad (4)$$

Whereas the electromagnetic torque, produced by the machine, can be defined by the next equation:

$$T_{em} = \frac{3PL_m}{2\sigma L_r L_s} (\psi_{rd} \psi_{sq} - \psi_{rq} \psi_{sd}) \quad (5)$$

where  $P$  is the pole pair number of the motor;  $R_s$  and  $R_r$  are the stator and rotor phase resistances, respectively;  $L_s$ ,  $L_r$  and  $L_m$  are the stator, rotor and mutual inductances, respectively; and  $\sigma$  is the total leakage factor.

Furthermore, the ARPs of the stator and rotor can be determined according to the next equations:

$$\left. \begin{aligned} P_s &= \frac{3}{2} (V_{sd} i_{sd} + V_{sq} i_{sq}) \\ Q_s &= \frac{3}{2} (V_{sq} i_{sd} - V_{sd} i_{sq}) \end{aligned} \right\} \quad (6)$$

$$\left. \begin{aligned} P_r &= \frac{3}{2} (V_{rd} i_{rd} + V_{rq} i_{rq}) \\ Q_r &= \frac{3}{2} (V_{rq} i_{rd} - V_{rd} i_{rq}) \end{aligned} \right\} \quad (7)$$

## III. Voltage Oriented Control Technique

The principle of the VOC consists of aligning the q-axis with the stator voltage space vector  $V_s$ , which means that  $V_s = V_{sq}$  and  $V_{sd} = 0$ .

From equation (1), since the stator is connected directly to the grid at constant AC voltage the stator flux is constant, thus, the term  $\frac{d\psi_s}{dt}$  is zero. Furthermore, considering that the voltage drop in the stator resistance is slight; consequently, the angle between the stator flux and the voltage vector almost is  $90^\circ$ , as demonstrated in Figure 1.

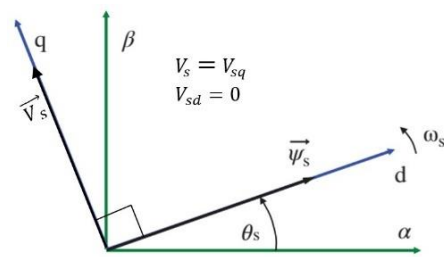


Figure 1. The phasor diagram of dq reference frame aligned with the stator voltage space vector

Thus, the equations (1,3,5 and 6) become as follows:

$$\left. \begin{aligned} V_{sd} &= 0 \\ V_{sq} &= \omega_s \psi_s \end{aligned} \right\} \quad (8)$$

$$\left. \begin{aligned} \psi_{sd} &= L_s i_{sd} + L_m i_{rd} \\ 0 &= L_s i_{sq} + L_m i_{rq} \end{aligned} \right\} \quad (9)$$

$$T_{em} = -\frac{3PL_m}{2\sigma L_r L_s} (\psi_{rq} \psi_{sd}) \quad (10)$$

$$\left. \begin{aligned} P_s &= \frac{3}{2} (V_{sq} i_{sq}) \\ Q_s &= \frac{3}{2} (V_{sq} i_{sd}) \end{aligned} \right\} \quad (11)$$

From the aforementioned equations, it can be noted that the current  $i_{rd}$  is proportional to the stator reactive power  $Q_s$  and that the current  $i_{rq}$  is proportional to the active stator power  $P_s$ . Accordingly, from the DFIG model by substituting equations (4) and (9) into equation (2), the rotor voltages can obtain as a function of stator flux and the rotor currents.

$$V_{rd} = R_r i_{rd} + \sigma L_r \frac{di_{rd}}{dt} - \omega_r \sigma L_r i_{rq} \quad (12)$$

$$V_{rq} = R_r i_{rq} + \sigma L_r \frac{di_{rq}}{dt} + \omega_r \sigma L_r i_{rd} + \omega_r \frac{L_m}{L_s} \psi_s \quad (13)$$

Consequently, by adopting similar PI controllers for both loops, and using the decoupling components between the dq axes. The equivalent closed-loop systems for currents can be represented as a second-order system by two poles and zero. Appropriate gains of the PI controllers are chosen as shown in Figure 2.

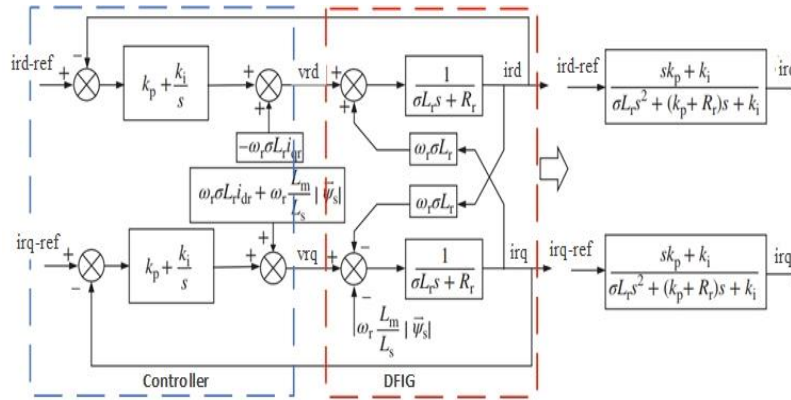


Figure 2. Inner closed-loop of rotor current control by PI controllers

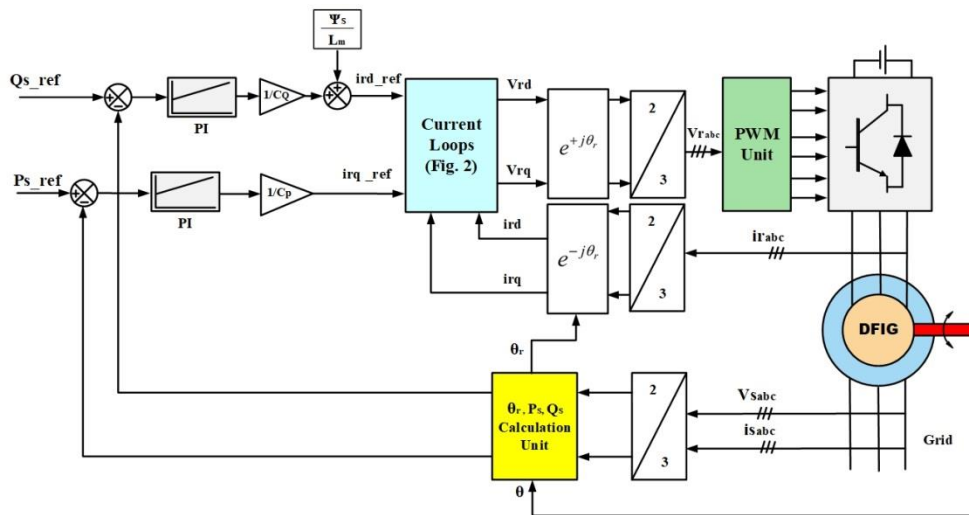


Figure 3. Overall block diagram of vector control technique

Next, it is possible to infer the external closed-loop of power control with PI controllers by substituting the

direct and quadrature rotor currents from equation (9) in equation (11).

$$P_s = -\frac{3}{2} \frac{L_m}{L_s} \omega_s \psi_s i_{rq} = C_p i_{rq} \quad (14)$$

$$Q_s = -\frac{3}{2} \frac{L_m}{L_s} \omega_s \psi_s \left( i_{rd} - \frac{\psi_s}{L_m} \right) = C_Q \left( i_{rd} - \frac{\psi_s}{L_m} \right) \quad (15)$$

It can be observed that the abridged closed-loop systems provide a first-order system that can be set by determining the proper gains of the PI controller. Consequently, the overall diagram of vector control for the DFIG is demonstrated in Figure 3.

#### IV. Direct Power Control Technique

In this study, the direct control technique for ARP is carried out based on the stator flux directing. The switching table is defined based on the ARP errors and the instantaneous location of the stator flux. The stator flux orientation method is adopted instead of the rotor flux orientation based on that the electrical components of the stator have less noise and harmonics compared to the electrical components of the rotor due to the discontinuous voltage applied to the rotor from the voltage converter RSC.

However, from equation (6), it is not possible to know how the injection of different rotor voltage vectors can affect the creation of desired  $P_s$  and  $Q_s$ . The stator voltage is fixed by the grid, whereas the stator current depends on the chosen rotor voltage vectors. Consequently, by substitution of DFIG model equations in equations (6) can be obtained follows the equations:

$$\left. \begin{aligned} P_s &= -\frac{3}{2} \frac{L_m}{\sigma L_r L_s} \omega_s \psi_{s_{xy}} \psi_{r_{xy}} \sin(\delta) \\ Q_s &= \frac{3}{2} \frac{\omega_s}{\sigma L_s} \psi_{s_{xy}} \left( \frac{L_m}{L_r} \psi_{r_{xy}} \cos(\delta) - \psi_{s_{xy}} \right) \end{aligned} \right\} \quad (16)$$

Where  $(\delta)$  is the phase shift between the stator and the rotor flux space vectors.

From equation (16) can notice the stator ARPs can be controlled by modifying the angle between the stator and rotor flux vectors and their amplitudes.

Fig. 4 illustrates the terms  $\psi_{r_{xy}} \sin(\delta)$ ,  $\psi_{r_{xy}} \cos(\delta)$ , stator and rotor flux space vector's locations.

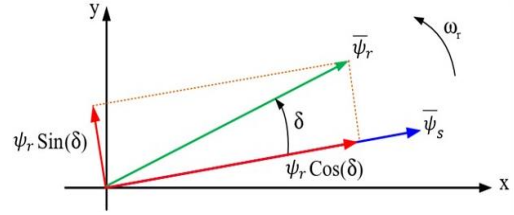


Figure 4. Phasor diagram of xy rotating reference frame with stator and rotor fluxes

The stator flux space vector position in the rotor reference frame is split into six sectors as shown in Figure 5.

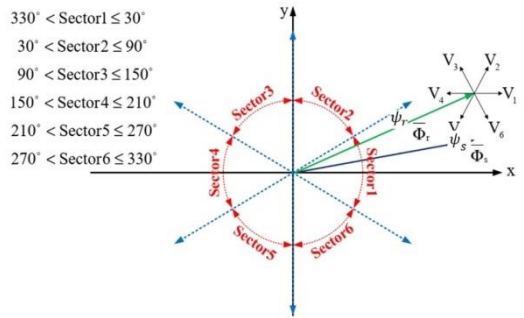


Figure 5. Distribution of the six sectors in xy rotating reference frame

##### IV.1. Voltage Vector Selection and Hysteresis Controllers

In the DPC technique, the required rotor voltage vector directly is select from  $P_s$  and  $Q_s$  errors, using hysteresis controllers. It determines the needed voltage vector to correct the errors in the controlled variables. The  $Q_s$  controller is based on a two-level hysteresis controller with  $H_Q$  hysteresis band, while the  $P_s$  controller employs a three-level hysteresis comparator with  $H_P$  hysteresis band. The schematic representation of these two controllers is shown in Fig. 6. Once the  $u_{P_s}$  and  $u_{Q_s}$  signals are defined employing the hysteresis controllers, together with the information about the stator flux vector position (i.e., the sector number), It can choose the rotor voltage vector from the switching table as illustrated in Table 1.

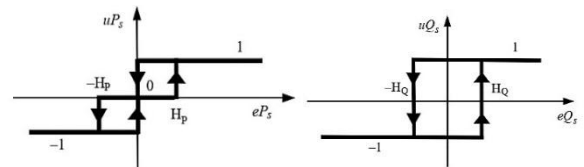


Figure 6. Active and reactive powers hysteresis controllers

Table 1. Switching table for DPC technique

$u_{Qs}$	1			-1		
$u_{Ps}$	1	0	-1	1	0	-1
Sector 1	$V_5$	$V_7$	$V_3$	$V_6$	$V_0$	$V_2$
Sector 2	$V_6$	$V_0$	$V_4$	$V_1$	$V_7$	$V_3$
Sector 3	$V_1$	$V_7$	$V_5$	$V_2$	$V_0$	$V_4$
Sector 4	$V_2$	$V_0$	$V_6$	$V_3$	$V_7$	$V_5$
Sector 5	$V_3$	$V_7$	$V_1$	$V_4$	$V_0$	$V_6$
Sector 6	$V_4$	$V_0$	$V_2$	$V_5$	$V_7$	$V_1$

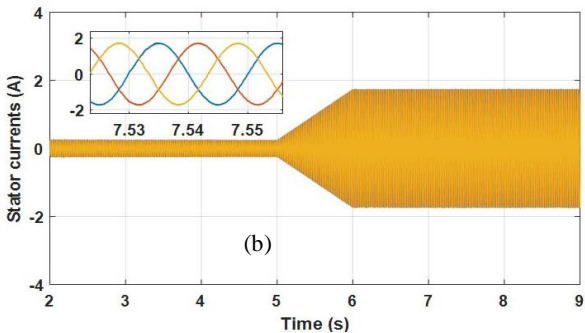
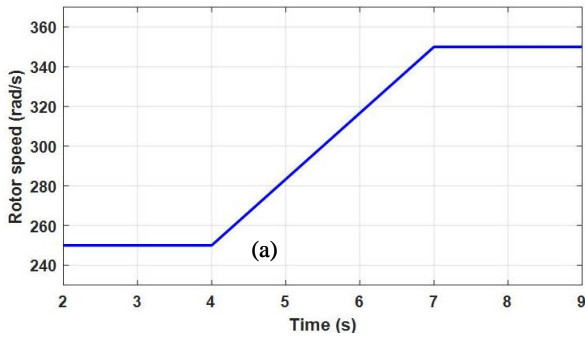
IV.2. Estimation of stator flux in  $xy$  rotating reference frame

The stator flux components are estimated from measured stator voltage and currents'  $\alpha$  and  $\beta$  components according to the following equations:

$$\left. \begin{aligned} \psi_{s\alpha} &= \int_0^t (V_{s\alpha} - R_s i_{s\alpha}) dt \\ \psi_{s\beta} &= \int_0^t (V_{s\beta} - R_s i_{s\beta}) dt \end{aligned} \right\} \quad (17)$$

The transformation matrix with the rotor angular position is employed to make the stator flux components rotate in  $xy$  rotating reference frame

$$\begin{bmatrix} \psi_{sx} \\ \psi_{sy} \end{bmatrix} = \begin{bmatrix} \cos(\theta) & \sin(\theta) \\ -\sin(\theta) & \cos(\theta) \end{bmatrix} \begin{bmatrix} \psi_{s\alpha} \\ \psi_{s\beta} \end{bmatrix} \quad (18)$$



Thus, the stator flux space vector angle which determines the sector number is calculated according to Fig. 5 by the following relationship

$$\theta_{\psi_{s-xy}} = \arctan 2 \left( \frac{\psi_{sy}}{\psi_{sx}} \right) \quad (19)$$

The control scheme of the DPC technique implemented in this study is demonstrated in Figure 7.

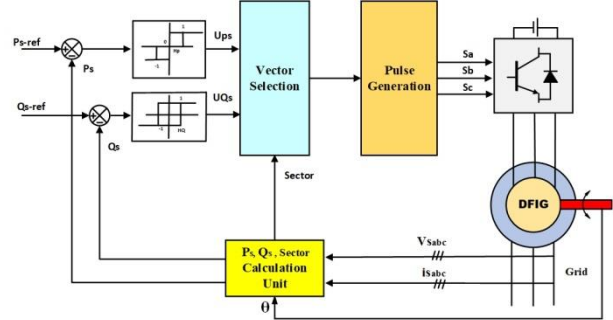
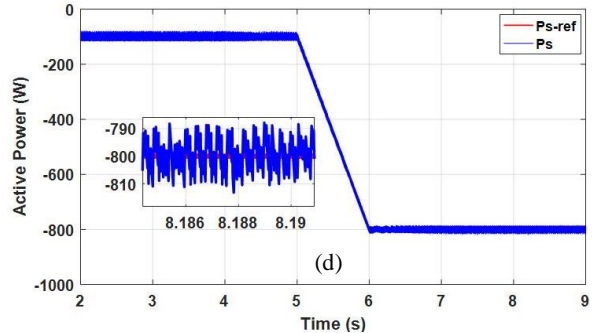
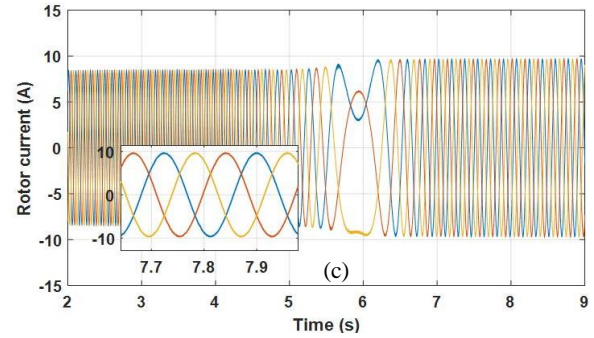


Figure 7. Block scheme of the DPC technique

V. Results and Discussion

The validity of the studied schemes was verified by the simulations using Matlab/Simulink. The simulation was carried out under various operating conditions to show the the studied techniques' performance.



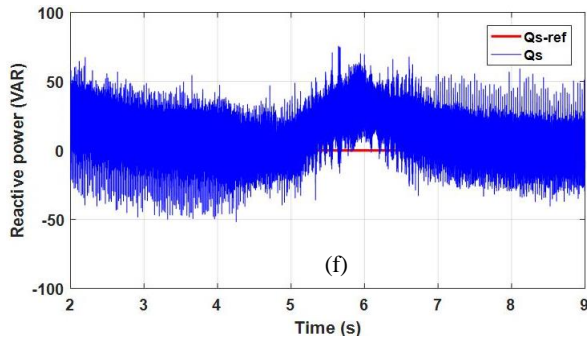


Figure 8. VOC technique responses for case 1

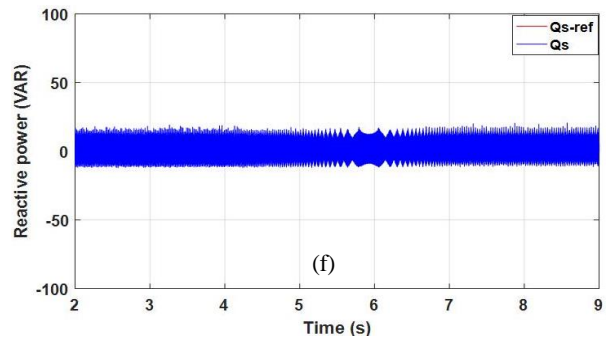
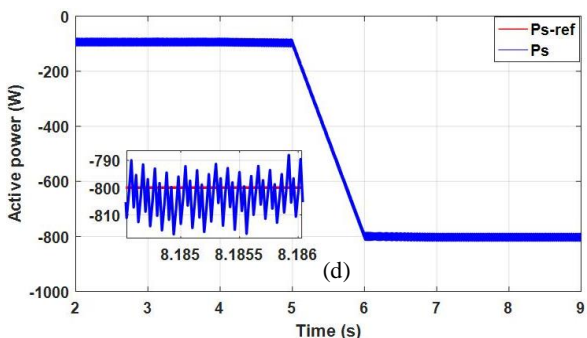
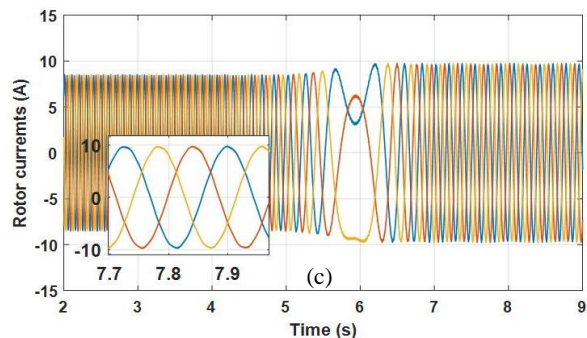
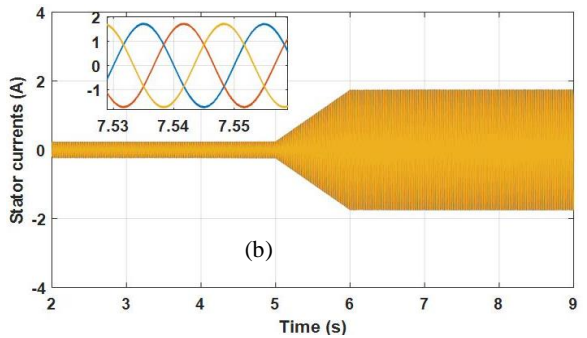
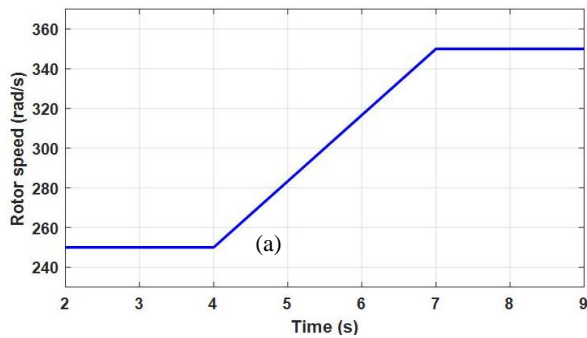


Figure 9. DPC technique responses for case 1



The Runge-Kutta method was used to solve differential equations. Sampling time is  $T_s = 20\mu s$  and the RSC converter switching frequency was set as 5KHz.

The nominal parameters of the DFIG are presented in Table 2. Both controls technique VOC and DPC are simulated and compared in the next cases:

Case 1: the rotor speed is increased from sub-synchronous to super-synchronous speed with ramp reference change of the active power.

Case 2: the rotor speed is set at sub-synchronous with the step reference change of the active power. In both cases, the reactive power is adjusted to zero to get a unity power factor at the grid side.

Table 2. Parameters of doubly fed induction generator

$P_n=1$ KW	$P=2$ pairs	$U_n=380$ V
$R_s=7.2 \Omega$	$L_s=0.28$ H	$R_r=1.35 \Omega$
$L_m=0.118$ H	$L_r=0.075$ H	$J=0.006$ kg.m <sup>2</sup>
$f_n=50$ Hz	$T_L=6.7$ N.m	$F=0.0046$ Nm.s

V.1. The performance at sub-synchronous and super-synchronous speed operation with ramp reference change of active power.

As shown in Figure 8 and 9, the rotor speed is sub-synchronous ( $\omega = 250$  rad/s) then at  $t = 4$  s it accelerating to become super-synchronous ( $\omega = 350$  rad/s). Also, the reference active power demand is increased from 100 to 800 watts at  $t = 5$  s.

From Figure 8 (f and d) and Figure 9 (f and d), it can be noticed the supremacy of the DPC technique in terms of response speed and reducing distortion occurring in the active and reactive power. Furthermore, in both techniques, balanced stator currents are obtained by maintaining a constant frequency equal to the grid frequency as illustrated in Figures 8 (b) and 9 (b).

V.2. Performance at sub-synchronous speed operation with the step reference change of active power.

In this test, a step variable reference active power is demanded at a sub-synchronous rotation speed. Figures 10 and 11 show the response of the ARP to both studied techniques. as noticed, the effectiveness and speed response of the DPC technique compared with the VOC technique. It can be seen the overshoot in the active power response with VOC technique and reactive power response variations according to active power variations. In the last comparison test, the total harmonic distortion (THD) of the stator current in each technique is evaluated by employing the Fast Fourier Transform (FFT) as seen in Figure 12. It can be seen that the THD for the DPC technique (THD = 1.01%) is low when compared with the VOC technique, and it's due to the difference and difficulty in choosing the optimal parameter values for PI controllers in the VOC technique.

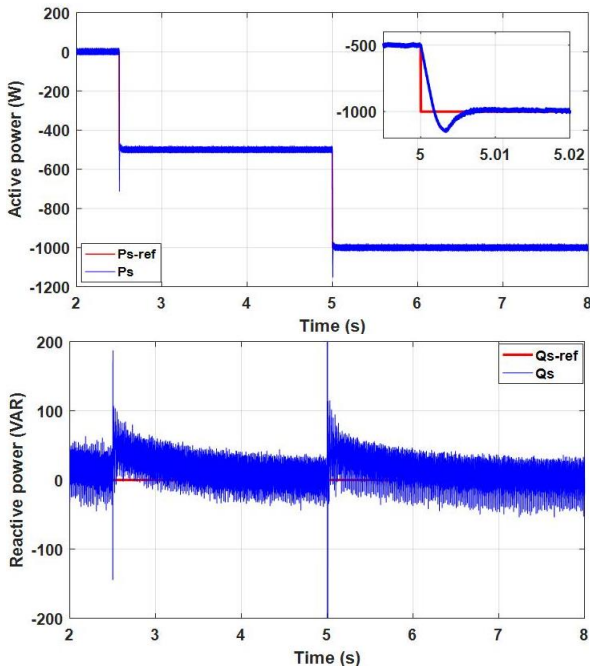


Figure 10. VOC technique responses for case 2

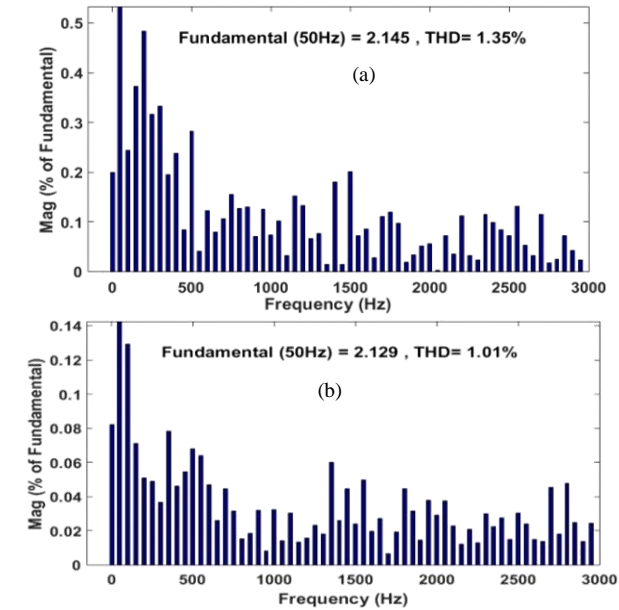
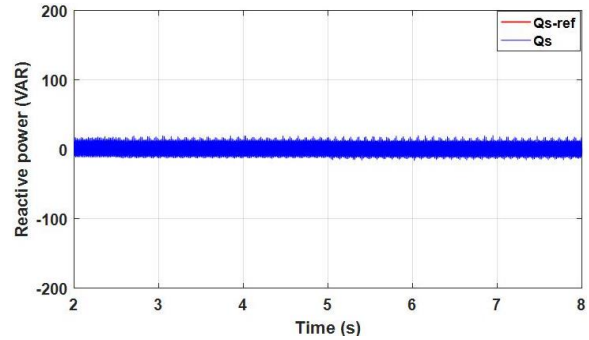
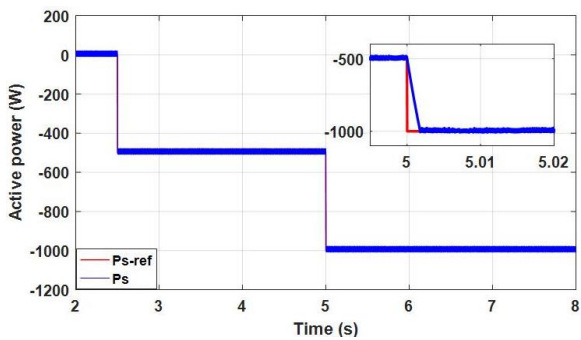


Figure 12. Stator current FFT analysis, (a) VOC, (b) DPC

After presenting the detailed simulation results indicating the superiority of the DPC technique, Table 3 reviews the key differences between the VOC technique and the DPC technique.

Table 3. Performance evaluation between DPC and VOC techniques

Indicators	DPC	VOC
Dynamic response	High	Low
Dependency on machine parameters	Very low	High
Power ripples	Medium	High
Switching frequency	Variable	Constant
Robustness	Medium	Low
Controllers	Tow hysteresis controllers	Four PI controllers
Control method	Directly controlled	Indirectly controlled by rotor currents
Park and Clark Transformations	No need	Needed

## VI. Conclusion

In this paper, the DPC and VOC techniques of DFIG in energy conversion systems were studied and simulated by MATLAB/SIMULINK. First, the theory of vector control by the stator voltage space vector orientation and how to calculate the parameters of PI controllers for the internal and external loops based on the mathematical model of DFIG was explained. Second, the stator flux orientation method is adopted instead of rotor flux orientation for the DPC technique using hysteresis controllers because the electrical components of the stator have less noise and harmonics compared to the electrical components of the rotor due to the discontinuous voltage applied to the rotor from the voltage converter RSC. Simulation results showed that the DPC technique presents a fast and good dynamic response and less harmonic distortion compared with the VOC technique. Moreover, the implementation of the DPC technique is simple and does not have the inherent complexity of the VOC technique. Additionally, extended studies of DFIG's control technologies can be achieved using advanced controllers such as the sliding mode controller and the fuzzy logic controller.

## References

- [1] R. Pena, J. C. Clare, and G. M. Asher, "Doubly fed induction generator using back-to-back PWM converters and its application to variable-speed wind-energy generation," *IEE Proceedings - Electric Power Applications*, Vol.143, Issue 3, 1996, pp. 231–241.
- [2] R. Pena, J. C. Clare, and G. M. Asher, "A doubly fed induction generator using back-to-back PWM converters supplying an isolated load from a variable speed wind turbine," *Electric Power Applications*, IEE Proceedings-, Vol. 143, Issue 5, 1996, pp. 380–387.
- [3] H. Akagi and H. Sato, "Control and performance of a doubly-fed induction machine intended for a flywheel energy storage system," *Power Electronics*, IEEE Transactions on, Vol. 17, Issue 1, 2002, pp. 109–116.
- [4] P. G. Holmes and N. A. Elsonbaty, "Cycloconverter-excited divided winding doubly-fed machine as a wind-power convertor," *Electric Power Applications*, IEE Proceedings B, Vol. 131, Issue 2, 1984, pp. 61–69.
- [5] A. Tapia, G. Tapia, J. X. Ostolaza, and J. R. Saenz, "Modeling and control of a wind turbine driven doubly fed induction generator," *Energy Conversion*, IEEE Transactions on, Vol. 18, Issue 2, 2003, pp. 194–204.
- [6] T. Noguchi, H. Tomiki, S. Kondo, and I. Takahashi, "Direct power control of PWM converter without power-source voltage sensors," *IEEE Trans. Ind. Appl.*, Vol. 34, Issue 3, 1998, pp. 473–479.
- [7] H. Nian, Y. Song, P. Zhou, S. S. Member, and Y. He, "Improved Direct Power Control of a Wind Turbine Driven Doubly Fed Induction Generator During Transient Grid Voltage Unbalance," *IEEE Transactions on Energy Conversion*, Vol. 26, Issue 3, 2011, pp. 976–986.
- [8] B. Nait-kaci, M. L. Doumbia, K. Agbossou and A. Yousif, "Active and reactive power control of a doubly fed induction generator for wind applications," *IEEE EUROCON 2009, St.-Petersburg, 2009*, pp. 2034-2039.
- [9] Muller S, Deicke M, De Doncker RW, "Doubly fed induction generator systems for wind turbines," *IEEE Industry Applications Magazine*, Vol.8, Issue 3, 2002, pp. 26-33.
- [10] Pena R, Clare JC, Asher GM, " A doubly-fed induction generator using two back-to-back PWM converters and its application to variable speed wind energy system," *IEE*, Vol.143, 1996, pp. 231-241.
- [11] T. Samina, S. Ramalyer and A. B. Beevi, "Dynamic behavior of wind driven doubly fed induction generator with rotor side control for wind power application," *2017 International Conference on Energy, Communication, Data Analytics and Soft Computing (ICECDS)*, Chennai, 2017, pp. 2470-2475.
- [12] A. R. Kumhar, "Vector Control Strategy to Control Active and Reactive Power of Doubly Fed Induction Generator Based Wind Energy Conversion System," *2018 2nd International Conference on Trends in Electronics and Informatics (ICOEI)*, Tirunelveli, 2018, pp. 1-9.
- [13] S. Seman, J. Niiranen, & A. Arkkio, "Ride-Through Analysis of Doubly Fed Induction Wind-Power Generator Under Unsymmetrical Network Disturbance." *Power Systems*, 21, IEEE Transactions, Issue 4, 2006, pp. 1782-1789.
- [14] Bakouri, Anass, et al. "A complete control strategy of DFIG connected to the grid for wind energy conversion systems." *2015 3rd International Renewable and Sustainable Energy Conference (IRSEC)*. IEEE, 2015.
- [15] E. Tremblay, S. Atayde, and A. Chandra, "Comparative Study of Control Strategies for the Doubly Fed Induction Generator in Wind Energy Conversion Systems: A DSP-Based Implementation Approach," *Sustainable Energy*, IEEE Transactions on, Vol. 2, Issue 3, 2011, pp. 288–299.
- [16] R. Datta and V. T. Ranganathan, "Direct power control of gridconnected wound rotor induction machine without rotor position sensors," *Power Electronics*, IEEE Transactions on, Vol. 16, Issue 3, 2001, pp. 390–399.
- [17] S. Massoum, A. Meroufel, A. Massoum, P. Wira, "A direct power control of the doubly-fed induction generator based on the SVM Strategy," *Elektrotehniški Vestnik*, Vol. 84, Issue 5, 2017, pp. 235–240.
- [18] A. Ben Amar, S. Belkacem, T. Mahni, " Direct torque control of a doubly fed induction generator," *International Journal of Energetica*, Vol. 2, Issue 1, 2017, pp. 11–14.